JOURNAL OF VIROLOGY, May 2005, p. 5979–5987 Vol. 79, No. 10
0022-538X/05/$08.00+0 doi:10.1128/JVI.79.10.5979–5987.2005

Characterization of the Interaction of Lassa Fever Virus with Its Cellular Receptor α-Dystroglycan

Stefan Kunz,[1]* Jillian M. Rojek,[1] Mar Perez,[1] Christina F. Spiropoulou,[2] and Michael B. A. Oldstone[1]

Division of Virology, Department of Neuropharmacology, The Scripps Research Institute, La Jolla, California 92037,[1] and Special Pathogens Branch, Centers for Disease Control and Prevention, Atlanta, Georgia 30333[2]

Received 30 September 2004/Accepted 23 December 2004

The cellular receptor for the Old World arenaviruses Lassa fever virus (LFV) and lymphocytic choriomeningitis virus (LCMV) has recently been identified as α-dystroglycan (α-DG), a cell surface receptor that provides a molecular link between the extracellular matrix and the actin-based cytoskeleton. In the present study, we show that LFV binds to α-DG with high affinity in the low-nanomolar range. Recombinant vesicular stomatitis virus pseudotyped with LFV glycoprotein (GP) adopted the receptor binding characteristics of LFV and depended on α-DG for infection of cells. Mapping of the binding site of LFV on α-DG revealed that LFV binding required the same domains of α-DG that are involved in the binding of LCMV. Further, LFV was found to efficiently compete with laminin α1 and α2 chains for α-DG binding. Together with our previous studies on receptor binding of the prototypic immunosuppressive LCMV isolate LCMV clone 13, these findings indicate a high degree of conservation in the receptor binding characteristics between the highly human-pathogenic LFV and murine-immunosuppressive LCMV isolates.

Several severe hemorrhagic fevers, including Lassa fever (LF) and Argentinian, Bolivian, and Venezuelan hemorrhagic fevers, are caused by arenaviruses (7). Among these, LF affects by far the largest number of people, with over 200,000 infections per year and several thousand deaths (37). The natural reservoir of Lassa fever virus (LFV) is the rodent *Mastomys natalensis* (40), and LF is endemic in Western Africa (38). The fatality rate of LF in hospitalized patients is >15% (39) and can rise to more than 50% in some outbreaks (14). In recent years, air travel of individuals incubating LFV resulted in the import of LF cases into the United States, Europe, Japan, and Canada (15, 20, 23, 45), with the potential to place such populations at risk.

LFV is classified within the Old World arenavirus group and is closely related to lymphocytic choriomeningitis virus (LCMV), the prototypic member of the *Arenavirus* family (7). The bisegmented negative-strand genome of LFV consists of two single-stranded RNA species: the larger segment encodes the virus polymerase (L) and a small zinc finger motif protein (Z); the smaller RNA segment encodes the virus nucleoprotein (NP) and glycoprotein precursor (GPC). GPC is processed into the peripheral glycoprotein GP1 and the transmembrane glycoprotein GP2 by the protease SKI-1/S1P (33). GP1 of arenaviruses is implicated in receptor binding (6, 42), and GP2 is structurally similar to the fusion-active membrane-proximal portions of the glycoproteins of other enveloped viruses (16).

The incubation period of LF is 7 to 18 days, followed by fever, weakness, and general malaise. A majority of patients develop cough, headache, sore throat, and gastrointestinal manifestations. Signs of increased vascular permeability such as facial edema and pleural effusions indicate a poor prognosis (39). In lethal cases, deterioration is rapid with progressive signs and symptoms of pulmonary edema, respiratory distress, and shock, accompanied by bleeding from mucosal surfaces (39). A highly predictive factor for disease outcome is the extent of viremia. Patients developing a fatal LFV infection have higher viral loads at time of hospitalization and are unable to limit viremia. In contrast, survivors have lower viral load and clear the virus (26).

Despite the widespread viral replication and development of shock in terminal stages of the disease, histological examination of LF patients shows surprisingly little cellular damage and only a modest or negligible infiltration of inflammatory cells (60). This finding suggests that there is failure of the host's antiviral immune response in these critically ill patients. In lethal LF cases, necrosis was found predominantly in the marginal zone of the splenic periarteriolar lymphocytic sheath (60). Interestingly, a similar picture of infection of cells in the marginal zone and loss of splenic architecture is also observed in mice infected with immunosuppressive isolates of LCMV (41, 46, 49). With immunosuppressive LCMV isolates, there is extensive infection of dendritic cells (DCs) (46). While there is no data for in vivo LFV infection in humans, in vitro infection of human DCs with LFV alters DC function (2, 35).

α-Dystroglycan (α-DG) has been identified as the first cellular receptor for LFV, LCMV, and clade C New World arenaviruses (8, 53). Initially encoded as a single protein, DG is cleaved into α-DG, a peripheral protein, and β-DG, a membrane protein (12, 13, 22). DG is expressed in most developing and adult tissues (10) and plays a critical role in cell-mediated assembly of basement membranes (18, 19, 34, 63). α-DG is expressed in a wide variety of human cells, among them cell types that play a crucial role in LF pathogenesis in humans, like, e.g., DCs (2, 35, 46) and different types of vascular endothelial cells (5, 21, 48, 59, 65). While there is a good correlation

* Corresponding author. Mailing address: Division of Virology, Department of Neuropharmacology, The Scripps Research Institute, 10550 N. Torrey Pines Rd., La Jolla, CA 92037. Phone: (858) 784-9447. Fax: (858) 784-9981. E-mail: stefanku@scripps.edu.

between α-DG expression and susceptibility to LFV infection for most of the cell types studied so far, skeletal muscle, which has high α-DG expression levels, is not a major in vivo target for LFV. The reason for this is unknown and may also be related to a block in viral replication other than cell attachment and/or entry.

At the extracellular site, α-DG undergoes high-affinity interactions with the extracellular matrix (ECM) proteins laminin-1, laminin-2, agrin, and perlecan (12, 13, 17, 56) and with neurexins (54). α-DG is noncovalently associated with the membrane-spanning β-DG. At the sacrolemma in muscle, β-DG associates intracellularly with dystrophin, which serves as a molecular link to the actin-based cytoskeleton. In nonmuscle tissues, dystrophin is replaced by its autosomal homologue utrophin (24, 29, 36). In addition to its role in cell-ECM adhesion (3, 4, 5, 24, 29), a growing body of evidence indicates that DG plays an important role in cellular signal transduction (9, 25, 50, 51, 52, 66).

Immunosuppressive strains and variants of LCMV bind to α-DG with very high affinity (30, 31, 46, 49), which is crucial for their ability to infect DCs and Schwann cells to cause a generalized immunosuppression (46, 49) and to block myelin formation (44), respectively. We have suggested elsewhere that the inability to control LFV loads and to mount a sufficient antiviral immune response to control infection may be the result of LFV-DC interaction (46, 47), while the common sensory neuropathy that occurs frequently in individuals who recover from LFV may be the result of LFV-Schwann cell interactions (44).

The present study analyzed the interaction of LFV with its cellular receptor α-DG. It was found that LFV binds α-DG with high affinity and depends on α-DG for infection of cells. LFV binding was noted to involve the same structures of α-DG implicated in binding to LCMV. LFV and the prototypic immunosuppressive LCMV isolate LCMV cl-13 efficiently compete with laminin α1 and α2 chains for α-DG binding. These findings indicate a high degree of conservation in the receptor binding characteristics between the highly pathogenic LFV and immunosuppressive isolates of LCMV.

MATERIALS AND METHODS

Proteins, antibodies, cell cultures and viruses. α-DG purified from rabbit skeletal muscle was biotinylated with the reagent NHS-X-biotin (Calbiochem), and its biological activity was verified as described previously (31). Monoclonal antibodies (MAbs) anti-LCMVGP2 83.6 and 33.6 recognize a common epitope on GP2 that is highly conserved among arenaviruses and have been described elsewhere (42, 61), as well as polyclonal rabbit antibody AP83 against β-DG (18). Horseradish peroxidase (HRP)-conjugated anti-mouse immunoglobulin G (IgG) and anti-rabbit IgG were from Pierce (Rockford, IL). Phycoerythrin (PE)-conjugated goat anti-mouse IgG was from Jackson Immuno-Research Laboratory (West Grove, PA).

The origin, passage, and characteristics of LCMV clone 13 and WE2.2 have been described elsewhere (1, 11, 58). Seed stocks of all viruses were prepared by growth in BHK-21 cells. Purified virus stocks were produced and virus titers determined as described previously (11). LFV Josiah was grown in Vero-E6 cells, polyethylene glycol precipitated and γ-inactivated at the Centers for Disease Control and Prevention, Atlanta, GA.

Immunoblotting and VOPBA. Purified viruses or total cellular protein was lysed in preheated (95°C) sodium dodecyl sulfate-polyacrylamide gel electroporesis (SDS-PAGE) sample buffer: 2% (wt/vol) SDS, 50 mM Tris-HCl, pH 6.8, 100 mM dithiothreitol. Proteins were separated by gel electrophoresis and transferred to nitrocellulose. After blocking in 5% (wt/vol) skim milk powder in phosphate-buffered saline (PBS), membranes were incubated with the primary antibody MAb 83.6 anti-LCMVGP2 (1:1,000) or polyclonal rabbit antibody AP83 against β-DG (1:1,000) in 2% (wt/vol) skim milk powder, PBS for 12 h at 6°C. After several washes in PBS, 0.1% (wt/vol) Tween 20 (PBST), the secondary antibody coupled to peroxidase was applied 1:5,000 in PBST for 1 h at room temperature. Blots were developed by enhanced chemiluminescence (ECL) using Super Signal West Pico ECL substrate (Pierce), and signals were recorded on autoradiographic film (Kodak, Rochester, N.Y.). The virus overlay protein binding assay (VOPBA) was performed as described previously (8). For comparison of the binding affinities for purified α-DG from skeletal muscle between LFV and LCMV cl-13, a log dilution of purified α-DG from rabbit skeletal muscle was made and 1, 0.1, 0.01, and 0.001 μg per lane was subjected to SDS-PAGE. The protein was transferred to nitrocellulose and probed for virus binding, using LFV and LCMV clone 13 in concentrations of 1×10^7 PFU/ml. Bound virus was detected by the monoclonal antibodies 33.6 and 83.6 (undiluted hybridoma supernatant), using ECL.

Binding of biotinylated α-DG and to LCMV variants. To test binding to biotinylated α-DG, γ-inactivated LFV, LCMV cl-13, and WE2.2 were immobilized in (enzyme immunoassay/radioimmunoassay) high-bond microtiter plates (Corning) and incubated with the indicated concentrations of biotinylated α-DG. Bound biotinylated α-DG was detected with peroxidase-conjugated streptavidin (Pierce) in a color reaction using ABTS [2,2′-azinobis(3-ethylbenzthiazolinesulfonic acid)] substrate. Optical density at 405 nm (OD_{405}) was recorded in an enzyme-linked immunosorbent assay (ELISA) reader. For the determination of specific binding, background binding to bovine serum albumin (BSA) was subtracted.

Transfection and expression of recombinant proteins. HeLa cells were transfected with the expression vectors, using Lipofectamine (GIBCO BRL). Cells were plated at 2×10^5 cells per well in six-well plates and kept at 37°C, 5% (vol/vol) CO_2 for 16 h. Plasmid DNA at 2 μg was diluted in 100 μl OPTIMEM (GIBCO BRL) mixed with 10 μl Lipofectamine dissolved in 100 μl OPTIMEM. The DNA-Lipofectamine mixture was incubated at room temperature for 20 min and then diluted to 1 ml with OPTIMEM. Cells were washed three times with OPTIMEM prior to addition of the DNA-lipofectamine mixture. Cultures were incubated for 5 h at 37°C in 5% (vol/vol) CO_2, the DNA-lipofectamine was removed, and fresh medium was added. Cells were kept for 24 to 48 h in 5% (vol/vol) CO_2. Transfections with the pC-EGFP (enhanced green fluorescent protein) reporter construct resulted in 20 to 30% transfected cells.

Flow cytometry. HeLa cells were transfected with pC-LFVGP and empty vector, using Lipofectamine as outlined above. To reduce cytotoxicity, cells were exposed to the Lipofectamine-DNA mixture for only one hour, resulting in circa 15 to 20% transfected cells, as assessed with the EGFP reporter construct. Forty-eight hours postinfection/transfection, cells were detached with enzyme-free cell dissociation solution (Sigma) and resuspended in fluorescence-activated cell sorting (FACS) buffer (1% [vol/vol] fetal bovine serum, 0.1% [wt/vol] sodium azide, PBS). For cell surface staining for LFVGP, cells were incubated with MAb 83.6 anti-LCMVGP2 (1:200 in FACS buffer) for 1 h on ice. Cells were then washed three times in FACS buffer and labeled with a PE-conjugated goat anti-mouse IgG (1:200 in FACS buffer) for 45 min on ice in the dark. After three wash steps in FACS buffer, cells were fixed with 4% (wt/vol) paraformaldehyde, PBS for 10 min at room temperature, washed three times with PBS, and analyzed with a FACSCalibur flow cytometer (Becton Dickinson, San Jose, CA) using Cell Quest software.

Generation of VSV pseudotypes. Recombinant vesicular stomatitis virus (VSV) strains pseudotyped with LFVGP or VSVGP were generated as described previously (43). Briefly, HEK293T cells were transfected with pC-LFVGP, pC-VSVGP, or pC-EGFP using Lipofectamine. Thirty-two hours posttransfection, cells were infected with VSVΔG* (55) at a multiplicity of infection (MOI) of 3 PFU/cell. After one hour, cells were extensively washed, fresh medium was added, and the cells were cultured for 20 h at 37°C, 5% CO_2. Supernatants were collected, cleared by centrifugation, and frozen at −70°C. Virus titers were determined by infection of HeLa cell monolayers. HeLa cells were grown in 96-well plates and infected with 100 μl of serially diluted virus stocks for one hour. The inoculum was removed, cells were washed twice with medium, and fresh medium was added. After 24 h, EGFP-positive cells were counted under an inverted fluorescence microscope. Doublets of infected cells were counted as one infectious unit (IU).

Blocking of infection of cells with VSVΔG*-LFVGP by inactivated LFV. For blocking, HeLa cells in 96-well plates (2×10^3 cells/well) were incubated with the indicated concentration of γ-inactivated LFV or Amapari in a total volume of 100 μl/well in 50% OPTIMEM–PBS. Two hundred infectious units of either VSVΔG*-LFVGP or VSVΔG*-VSVGP was mixed with the same concentrations of γ-inactivated LFV or Amapari in a total volume of 100 μl OPTIMEM-PBS, and the inoculum was added to the cells. After 45 min of incubation at 37°C, 5%

CO_2, supernatants were removed and cells were washed four times with medium and incubated for 24 h. Infection was quantified by immunofluorescence as described above.

Infection of ES cells with VSV pseudotypes. Mouse $DG^{-/-}$ and $DG^{+/-}$ embryonic stem (ES) cells maintained as described previously (18) were plated in gelatin-pretreated 96-well plates at a density of 10^4 cells/well. Adenovirus (AdV) vector-mediated gene transfer of wild-type DG and the DG deletion mutants DGI (ΔH30-R168), DGD (ΔC182-H315), DGE (ΔH30-A316), DGF (ΔT317-P408), and DGG (ΔG409-S485) (30) was performed as described previously (8). After 48 h, the indicated IU of VSV pseudotypes were added to AdV-transfected $DG^{-/-}$ ES cells, as well as untreated control $DG^{-/-}$ and $DG^{+/-}$ cells at and incubated for 1 h at 37°C. The viral particles were removed, cells were washed twice with Dulbecco's modified Eagle's medium, and fresh medium was added. After the time points indicated, infected cells were quantified by fluorescence microscopy.

Binding of LCMV and LFV to α-DG-Fc fusion proteins in ELISA. The α-DG-Fc fusion proteins DGFc1 (amino acids [aa] 30 to 181), DGFc2 (aa 30 to 316), DGFc3 (aa 30 to 408), DGFc4 (aa 30 to 485), and full-length α-DG-Fc (DGFc5; aa 30 to 653) were expressed and purified as described previously (30). Purified α-DG-Fc fusion proteins (20 μg/ml in PBS) were immobilized in microtiter plates. Nonspecific binding was blocked by adding 200 μl/well 1% (wt/vol) BSA–PBS and incubation for 1 h at room temperature. γ-inactivated LFV was applied in a concentration of 10^7 PFU/ml in 1% (wt/vol) BSA–PBS for 12 h at 6°C. For detection of bound virus, MAb 83.6 anti-LCMVGP2 (purified IgG, 20 μg/ml) was used in 1% BSA–PBS. Bound primary antibody was detected with peroxidase-conjugated secondary antibody in a color reaction using ABTS substrate. OD_{405} was recorded in an ELISA reader. For the determination of specific binding, background binding to BSA was subtracted.

Competition of the binding of LFV and LCMV to α-DG with ECM proteins. α-DG, purified from rabbit skeletal muscle (28), was immobilized in microtiter plates. Nonspecific binding was blocked by adding 200 μl/well 1% (wt/vol) BSA–PBS and incubation for 1 h at room temperature. After a brief rinse with 20 mM HEPES, 150 mM NaCl, pH 7.5, the plate was incubated for 1 h in laminin-overlay buffer (TLBB): 20 mM HEPES, 150 mM NaCl, pH 7.5, containing 1 mM $CaCl_2$ and 1 mM $MgCl_2$ in 1% BSA at room temperature. The indicated concentrations of laminin-1 (mouse isolated from EHS GIBCO), merosin (human GIBCO), fibronectin (human GIBCO), and BSA were incubated for 4 h at room temperature. γ-inactivated LFV and LCMV cl-13 were applied in a concentration of 10^7 PFU/ml in TLBB containing the blocking proteins for 12 h at 6°C. Bound virus was detected as described above. For displacement experiments, 10^7 PFU/ml γ-inactivated LFV and LCMV cl-13 were preincubated with immobilized α-DG in TLBB for 12 h at 6°C, followed by the indicated concentrations of laminin-1, merosin, fibronectin, and BSA in TLBB for four hours at room temperature. Bound virus was subsequently detected as described above.

RESULTS

LFV binds its cellular receptor α-DG with high affinity. To compare the receptor binding affinities of LFV and the prototypic immunosuppressive LCMV variant clone 13 (cl-13), binding of purified viruses (Fig. 1A) to a log dilution of purified α-DG was tested in a VOPBA (Fig. 1B). These experiments revealed α-DG binding affinities within the same order of magnitude for both viruses (Fig. 1B). For a more quantitative analysis of the LFV binding to α-DG, an ELISA-format assay was utilized. Briefly, purified LFV, LCMV cl-13, and LCMV WE2.2, which does not bind to α-DG, were immobilized in microtiter plates and binding of biotinylated α-DG was determined. Half-maximal binding to LFV was observed with 6.8 (± 2.4) nM biotinylated α-DG and to LCMV cl-13 with 0.8 (± 0.4) nM, respectively (Fig. 1C), while no significant binding to α-DG was observed with LCMV WE2.2. These data show that LFV binds to its cellular receptor α-DG with an affinity that is in the low-nanomolar range, similar to the binding affinities observed with LCMV cl-13 and other immunosuppressive isolates of LCMV (31).

Recombinant vesicular stomatitis virus pseudotyped with LFVGP adopts the receptor binding characteristics of LFV

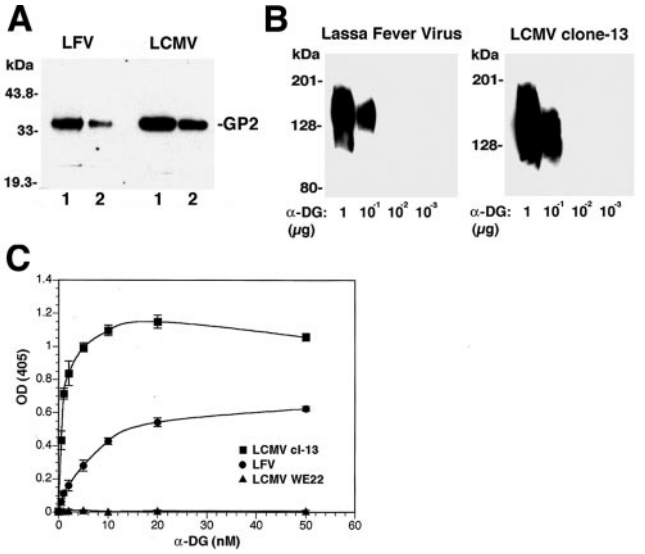

FIG. 1. LFV binds α-DG with high affinity. (A) Detection of viral GPs in purified LFV and LCMV. Purified LFV strain Josiah (inactivated by γ-irradiation) and LCMV cl-13 (10^7 PFU/ml each) were solubilized in SDS-PAGE buffer, and 40 μl (lanes 1) and 10 μl (lanes 2) of the samples were separated by SDS-PAGE and transferred to nitrocellulose. Blots were probed with MAb 83.6 anti-LCMVGP2, using a peroxidase-conjugated secondary antibody and enhanced chemiluminescence (ECL) for detection. Molecular masses are indicated. (B) Comparison of the binding affinities for α-DG of LFV and LCMV cl-13 by VOPBA. α-DG, purified from rabbit skeletal muscle, was diluted (1, 0.1, 0.01, 0.001 μg) and blotted to nitrocellulose. LFV and LCMV cl-13 were applied at the same concentration (10^7 PFU/ml). Bound virus was detected by monoclonal antibodies 33.6 and 86.6 that recognize conserved epitopes of LFV and LCMV GP2, using a peroxidase-conjugated anti-mouse IgG secondary antibody and enhanced chemiluminescence (ECL). (C) Binding of α-DG to LFV, LCMV cl-13, and LCMV WE2.2. LFV Josiah (circles), LCMV cl-13 (squares), and LCMV WE2.2 (triangles) were immobilized in a microtiter plate and incubated with biotinylated α-DG. Bound biotinylated or α-DG was detected with peroxidase-conjugated streptavidin in a color reaction using ABTS substrate. OD_{405} was recorded in an ELISA reader. For the determination of specific binding, background binding to BSA was subtracted (mean ± standard deviation; $n = 3$).

and depends on α-DG for infection of cells. Since LFV is a BSL4 pathogen, the use of live virus in the laboratory is restricted. In order to study the LFV-receptor interaction in host cells, we established a reporter gene cell culture assay using recombinant VSV that carries LFVGP in its surface. The availability of a reverse genetic system for VSV allowed the generation of recombinant viruses that contain reporter genes inserted in their genomes (32, 62). We used a recombinant VSV (VSVΔG*) in which the VSV G gene was replaced by a green fluorescent protein reporter gene (55). Viral particles released from VSVΔG*-infected cells incorporated heterologous viral GPs, provided in *trans*, into their lipid membranes during budding (27, 43, 57, 64). These pseudotyped viruses acquired the host range of the virus from which the heterologous GP was derived. For the expression of recombinant LFVGP in mammalian cells in *trans*, the cDNA of the GPC sequence derived from LFV strain Josiah was inserted into the eukaryotic expression vector pcAGGS, resulting in the construct pC-LFVGP. For an initial characterization of recombinant LFVGP, HeLa cells were transfected with either pC-LFVGP

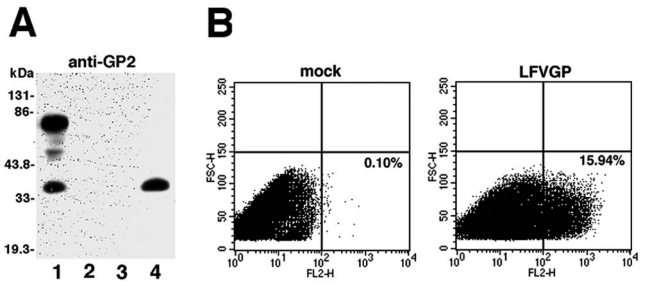

FIG. 2. Characterization of recombinant LFVGP. (A) Expression of recombinant LFVGP. HeLa cells were transfected with the expression construct pC-LFVGP (lane 1), pC-EGFP (lane 2), and empty vector (lane 3) using Lipofectamine. Two days after transfection, cells were lysed in SDS-PAGE sample buffer. As a positive control, a lysate of purified LFV virions (10^7 PFU/ml) was used (lane 4). Proteins were separated by SDS-PAGE, transferred to nitrocellulose, and analyzed by Western blot using MAb 83.6 anti-LCMVGP2. Bound primary antibody was detected with a peroxidase-conjugated secondary antibody using ECL for detection. Molecular masses are indicated. (B) Cell surface labeling of recombinant LFVGP. HeLa cells were transfected with pC-LFVGP (LFVGP) or empty vector (mock) as in panel A. Cell surface LFVGP was detected with MAb 83.6 anti-LCMVGP2 and a PE-conjugated secondary antibody to mouse IgG. For flow cytometry, a FACSCalibur flow cytometer was used. In histograms, the *y* axis represents cell numbers and the *x* axis represents fluorescence intensity (FL2-H for anti-mouse IgG–PE conjugate).

or a control construct, pC-EGFP, that contains an EGFP marker. Forty-eight hours after transfection, cells were lysed and total cell protein was analyzed by Western-blot analysis using MAb 83.6, which recognizes a highly conserved epitope present in GP2 of arenaviruses (61). Processed recombinant LFVGP2 exhibited a molecular mass similar to LFVGP2 present in LFV virions (Fig. 2A). The additional prominent band at a molecular mass of 75 kDa likely corresponds to the unprocessed GPC precursor and is absent from purified LFV (Fig. 2A, lane 4), indicating complete processing of LFVGP incorporated into virion particles. Cell surface expression of recombinant LFVGP was verified by immunostaining performed on live, nonpermeabilized cells transfected with LFVGP using flow cytometry (Fig. 2B). Together, these data indicate efficient expression, processing, and cell surface expression of recombinant LFVGP in human cell lines.

We pseudotyped the recombinant VSV variant VSVΔG*, which contains an EGFP reporter with the glycoproteins of LFV and VSV, using the strategy described in reference 43. Briefly, HEK293T cells were transfected with the expression construct pC-LFVGP, pC-VSVGP, or pC-EGFP, using Lipofectamine. Thirty-two hours after transfection, cells were infected with VSVΔG*. After 24 h, culture supernatants were collected. Monolayers of HeLa cells in a 96-well plates were infected with serial dilutions of VSVΔG*-LFVGP, VSVΔG*-VSVGP, and VSVΔG* from EGFP-transfected cells, which lack viral GP. At 20 h postinfection, EGFP-positive cells were counted under an inverted fluorescence microscope and titers were calculated. Doublets of EGFP-expressing cells were counted as one IU. For VSVΔG*-LFVGP, we obtained titers in the range of 1×10^5 to 8×10^5 IU/ml, for VSVΔG*-VSVGP, titers were 2×10^7 to 9×10^7 IU/ml, and for VSVΔG* lacking GP titers were typically 1×10^2 to 10×10^2 IU/ml. To address the question whether our VSVΔG*-LFVGP pseudotypes show the same receptor specificity as LFV, we blocked HeLa cells with an excess of γ-inactivated LFV prior to infection with either VSVΔG*-LFVGP or VSVΔG*-VSVGP. As a control, we used γ-inactivated Amapari, a clade B New World arenavirus that does not use α-DG as a cellular receptor (53). Infection with VSVΔG*-LFVGP but not VSVΔG*-VSVGP was significantly reduced by blocking with inactivated LFV but not Amapari (Fig. 3A), indicating similar receptor specificity of VSVΔG*-LFVGP and LFV.

To analyze the dependence of infection by VSVΔG*-LFVGP on α-DG, we made use of $DG^{-/-}$ mouse ES cells and their corresponding heterozygous $DG^{+/-}$ parental line (8, 18). $DG^{-/-}$ and $DG^{+/-}$ ES cells were incubated with either VSVΔG*-LFVGP or VSVΔG*-VSVGP, and infection was assessed after 24 h by detection of EGFP expression. To exclude the possibility that differential infection of $DG^{-/-}$ and $DG^{+/-}$ ES cells by VSVΔG*-LFVGP was due to factors not related to α-DG deficiency, we reconstituted DG expression in $DG^{-/-}$ ES cells. For this purpose, we infected $DG^{-/-}$ ES cells with

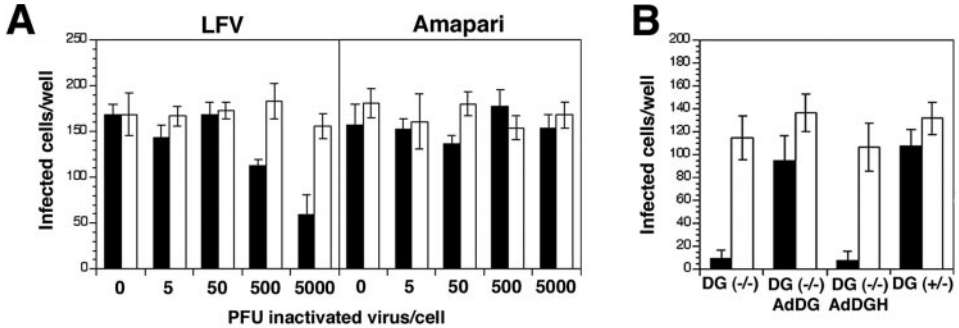

FIG. 3. Recombinant vesicular stomatitis virus pseudotyped with LFVGP adopts the receptor binding characteristics of LFV and depends on α-DG for infection. (A) Blocking of VSVΔG*-LFVGP infection by γ-inactivated LFV. HeLa cells cultured in 96-well plates were blocked with the indicated PFU/cell of γ-inactivated LFV or γ-inactivated Amapari. After incubation for two hours at 4°C, cells were infected with 200 IU of VSVΔG*-LFVGP (black bars) or VSVΔG*-VSVGP (white bars). Infection was assessed after 24 h by detection of the EGFP reporter in fluorescence microscopy. Data are EGFP-positive cells per well ($n = 3$; ± standard deviation). (B) Infection with LFV-PS depends on α-DG. $DG^{-/-}$ ES cells were infected with AdV vectors containing either wild-type DG or the deletion mutant DGH at an MOI of 10. After 48 h, AdV-infected cells as well as $DG^{-/-}$ and $DG^{+/-}$ ES cells cultured in parallel were infected with 200 IU of VSVΔG*-LFVGP or VSVΔG*-VSVGP and infection was assessed after 24 h as in panel B ($n = 6$; ± standard deviation).

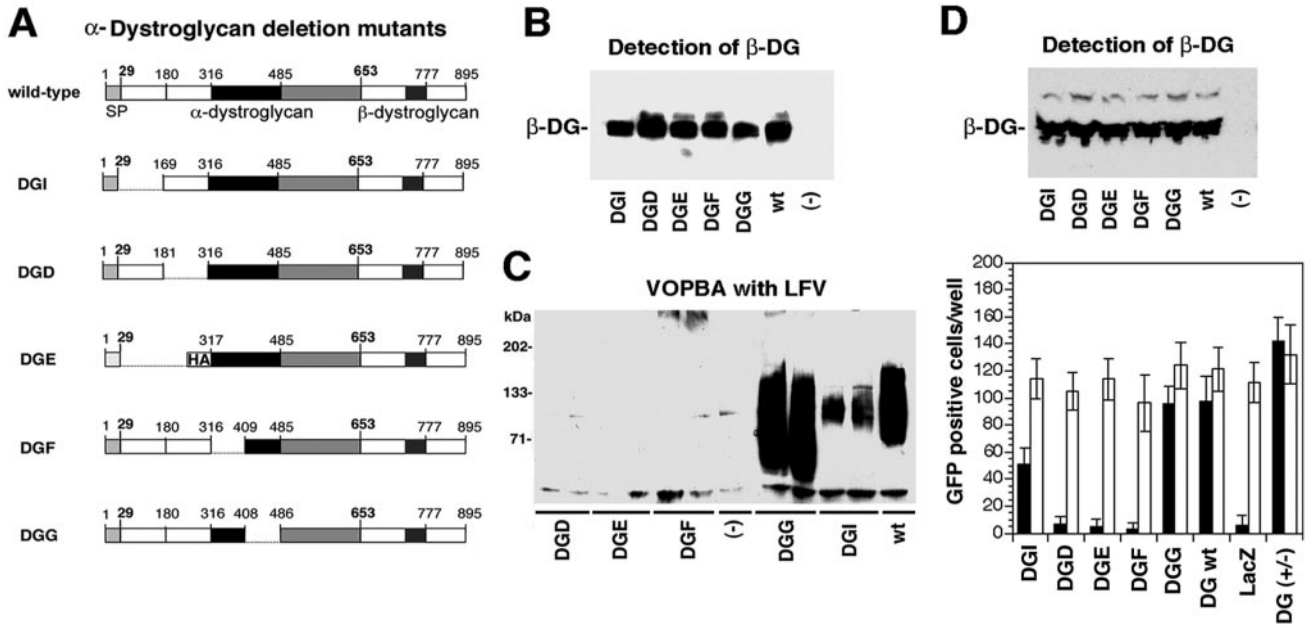

FIG. 4. Structures within amino acids 169 to 408 are required for LFV binding. (A) Schematic representation of the α-DG deletion mutants: The putative N-terminal subdomains (white), the mucin-type domain (black), and the C-terminal globular domain (gray) of α-DG are indicated. Amino acids 653 to 895 represent β-DG with the transmembrane domain (dark box). The influenza virus hemagglutinin (HA) epitope in DGE is indicated. (B) Expression of the α-DG deletion mutants. $DG^{-/-}$ ES cells were infected with AdV vectors containing the α-DG variants or green fluorescent protein (−). After 48 h, cells were lysed and samples subjected to jacalin affinity chromatography. Jacalin-bound glycoproteins were separated by SDS-PAGE, transferred to nitrocellulose, and probed with anti-β-DG. wt, wild type. (C) Binding of LCMV cl-13 and LFV to wild-type and deletion mutants of α-DG. Jacalin-bound glycoproteins (B) were subjected to VOPBA with 10^7 PFU/ml of LFV using MAb 83.6, anti-LCMVGP2, and enhanced chemiluminescence (ECL) for detection. (D) Reconstitution of LFV-PS infectivity in $DG^{-/-}$ ES cells by wild-type and deletion mutants of α-DG. $DG^{-/-}$ ES cells were infected with AdV vectors containing wild-type and deletion mutants of α-DG or a β-galactosidase reporter gene (LacZ) at an MOI of 10. After 48 h, transgene expression was verified by detection of β-DG in total cell protein in the Western blot. Cells cultured in parallel were infected with 200 IU (MOI = 0.01) of VSVΔG*-LFVGP (black bars) or VSVΔG*-VSVGP (white bars), and infection was assessed after 24 h as in panel B. Infection levels were assessed 24 h later by the detection of GFP-positive cells by immunofluorescence ($n = 6$; ± standard deviation).

AdV vectors containing wild-type DG or the α-DG deletion mutant DGH (ΔH30-S485), which lacks most of α-DG (30). Within 48 h after AdV-mediated gene transfer, which resulted in >80% of the cells expressing heterologous protein, cells were infected with the VSV pseudotypes. Infection with VSVΔG*-LFVGP and VSVΔG*-VSVGP was assessed after 24 h as described above. VSVΔG*-LFVGP infected $DG^{+/-}$ ES cells and $DG^{-/-}$ ES cells reconstituted with wild-type DG significantly more efficiently than $DG^{-/-}$ ES cells or $DG^{-/-}$ ES cells transfected with DGH (Fig. 3B). In contrast, VSVΔG*-VSVGP infected all cell types equally well. These data indicate that the reduced infection of $DG^{-/-}$ ES cells by VSVΔG*-LFVGP is due to lack of α-DG-mediated entry and not caused by a block in a later step of viral replication and/or reporter gene expression. Together, our data show that VSVΔG*-LFVGP adopts the receptor specificity of LFV and depends on α-DG for infection of cells.

The N-terminal globular domain and parts of the mucin-related domain of α-DG are involved in LFV binding. To map the LFV binding site on α-DG, we utilized a series of α-DG deletion mutants recently generated and characterized (30). The α-DG deletion mutants and wild-type DG (Fig. 4A) were transfected in $DG^{-/-}$ ES cells, using AdV vectors, and expression levels were verified by Western blot (Fig. 4B). For the analysis of virus binding, the α-DG variants were subjected to VOPBA with γ-inactivated LFV (Fig. 4C). Virus binding was only observed with DG variants containing amino acids 169 to 408, indicating that this part of α-DG is required for virus binding.

To test the α-DG deletion mutants for their ability to reconstitute virus infection in nonpermissive cells, we infected $DG^{-/-}$ ES cells with the AdV vectors carrying the α-DG deletion mutants and wild-type DG. Within 48 h after AdV-mediated gene transfer, transgene expression was verified by detection of β-DG in total cell lysates (Fig. 4D). AdV transfectants cultured in parallel were infected with VSVΔG*-LFVGP and VSVΔG*-VSVGP. Twenty-four hours later, infection was assessed by immunofluorescence detection of EGFP. Consistent with the binding data (Fig. 4C), only DG variants containing amino acids 169 to 408 were able to reconstitute VSVΔG*-LFVGP infection (Fig. 4D). As expected, VSVΔG*-VSVGP infected all transfectants equally well. Together, these data indicated that structures within amino acids 169 to 418 are required for the function of α-DG as a receptor for LFV.

In a complementary approach, we produced soluble α-DG fragments as fusion proteins with the Fc region of human IgG (Fig. 5A). The α-DG-Fc fusion proteins DGFc1 through DGFc5 were expressed in HEK293T cells and purified from cell lysates by protein A affinity chromatography as described previously (30). When analyzed by SDS-PAGE with Coomassie blue staining (Fig. 5B) and a Western blot using an anti-IgG

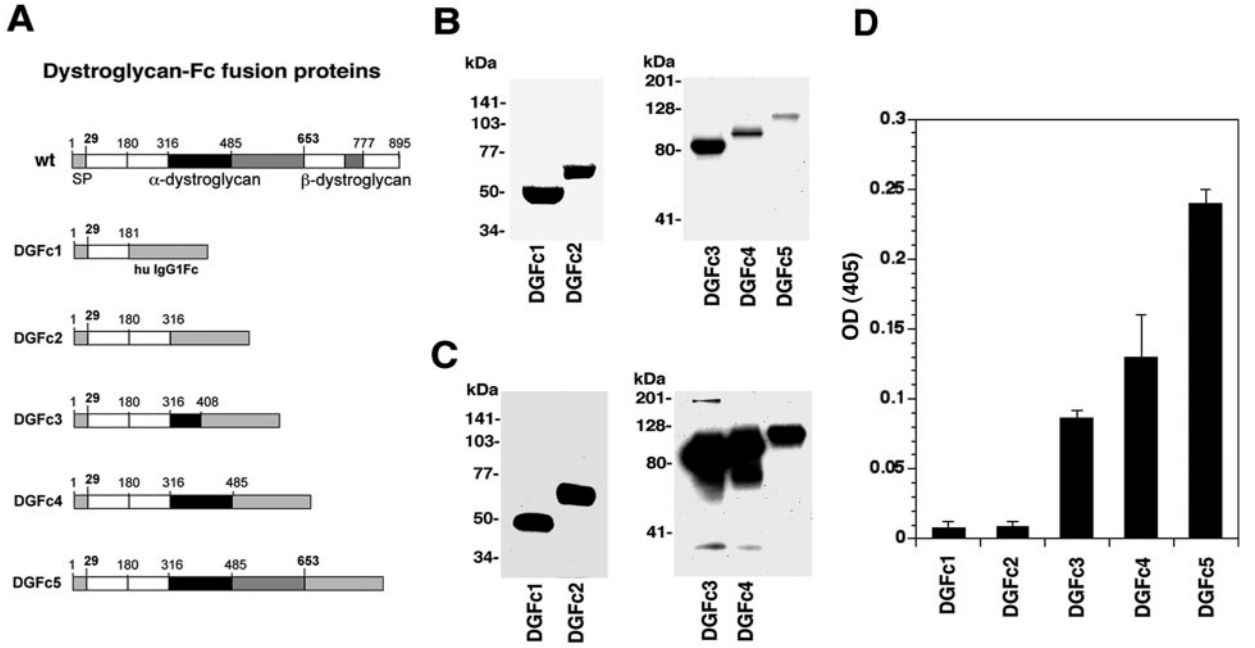

FIG. 5. Amino acids 169 to 408 of α-DG contain a high-affinity binding site for LFV and LCMV. (A) Schematic representation of the α-DG fragments fused to human IgG Fc. The putative domains of α-DG are depicted as in Fig. 4, and human IgG1Fc is indicated. wt, wild type. (B) Purified α-DG-Fc fusion proteins. The α-DG-Fc fusion proteins DGFc1 through -5 were expressed in HEK293T cells and purified by protein A affinity chromatography from cell lysates. Purified proteins were analyzed by SDS-PAGE with Coomassie blue staining (B) and by Western blot using an anti-human IgG Fc antibody (C). (D) Binding of LFV to the α-DG-Fc fusion proteins. Equal amounts of purified DGFc1 through -5 were immobilized in microtiter plates and incubated with 10^7 PFU/ml γ-inactivated LFV. Bound virus was detected with MAb 83.6 (anti-LCMVGP2) and a peroxidase-conjugated secondary antibody in a color reaction using ABTS substrate. OD_{405} was recorded in an ELISA reader. For the determination of specific binding, background binding to BSA was subtracted (mean ± standard deviation; $n = 3$).

Fc antibody (Fig. 5C), DGFc1 through -5 showed the expected apparent molecular masses. In an ELISA-format binding assay, DGFc3, DGFc4, and DGFc5 but not DGFc1 and DGFc2 specifically bound to LFV (Fig. 5D). Together, our findings indicate that structures within amino acids 169 to 408 of α-DG are required for high-affinity binding to LFV.

LFV and the immunosuppressive LCMV isolate cl-13 compete with laminin α1 and α2 chains for α-DG binding. Laminins containing α1 and α2 chains represent a major group of ECM proteins that undergo high-affinity interactions with α-DG in a wide variety of host tissues. Our previous studies demonstrated that the prototypic immunosuppressive LCMV isolate cl-13 can compete with laminin-1 and laminin-2 for α-DG binding (30, 44). To extend these studies, a quantitative analysis of the competition of LFV and LCMV cl-13 with laminin-1 and laminin-2, which bind to α-DG by their α1 and α2 chains, was performed. Virus binding to α-DG was blocked in a dose-dependent manner with increasing concentrations of laminin-1 and laminin-2, but not fibronectin, which does not use α-DG as a receptor (Fig. 6A). These data show that LFV and LCMV compete with the ECM proteins laminin-1 and laminin-2 for α-DG binding. When LFV and LCMV cl-13 were bound to α-DG prior to addition of soluble ECM proteins, neither of the two viruses could be significantly displaced (Fig. 6B). This indicates that the virus acts as a high-affinity multivalent ligand that binds irreversibly to its cellular receptor. Together, our data indicated that LFV and LCMV cl-13 can efficiently compete with laminin α1 and α2 chains for α-DG binding.

DISCUSSION

The present study investigated the interaction of LFV with its cellular receptor α-DG and revealed a high degree of similarity between the receptor binding characteristics of LFV and immunosuppressive isolates of LCMV. Like immunosuppressive strains and variants of LCMV, LFV binds α-DG with an affinity in the low-nanomolar range and depends on α-DG for infection of cells. The resemblance in binding affinity is reflected by overlapping binding sites for LFV and LCMV on α-DG. Further, LFV was found to compete efficiently with laminins containing α1 and α2 chains for α-DG binding.

The interaction of a virus with its cellular receptor(s) is the first and fundamental step for the virus-host cell relationship and thus provides a key determinant for both the tissue tropism and disease potential of a virus. The cellular receptor for LFV, LCMV, and clade C New World arenaviruses has been identified as α-DG (8, 53). Our earlier studies indicated a striking and consistent correlation between α-DG binding affinity, tissue tropism, and pathological potential of LCMV (30, 46, 49). LCMV strains and variants with high binding affinity to α-DG, like LCMV cl-13, replicate preferentially in the white pulp of the spleen and infect >75% of $CD11c^+$ and $DEC205^+$ DC, which express α-DG at their surface (46, 47). Their infection reduces their ability to act as antigen-presenting cells, resulting in an impairment of the antiviral T- or B-cell responses. The result is a generalized immunosuppression in the host. In contrast, strains and variants of LCMV with low binding affinity for α-DG localize primarily to the red pulp of

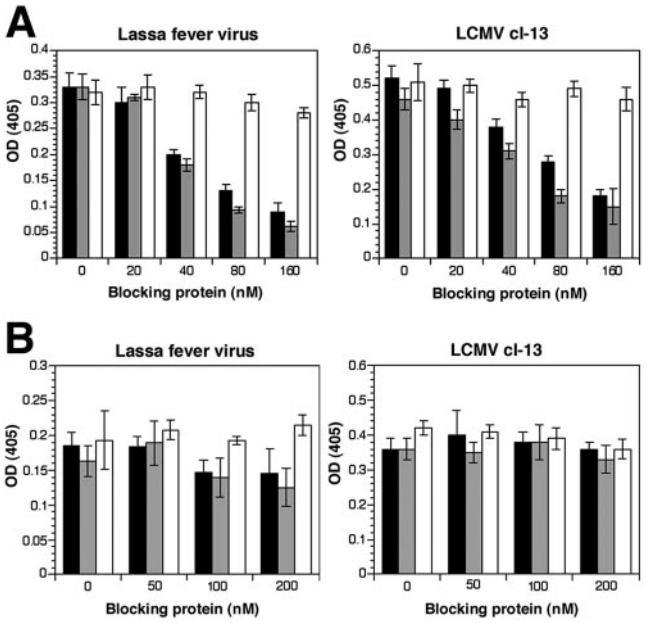

FIG. 6. LFV and LCMV cl-13 compete with laminin α1 and α2 chains for α-DG binding. (A) Blocking of virus binding to α-DG by laminin-1 and laminin-2. α-DG purified from rabbit skeletal muscle was immobilized in microtiter plates and blocked with the indicated concentrations of laminin-1 (black), laminin-2 (gray), and fibronectin (white) for 4 h at room temperature. Inactivated LFV and LCMV cl-13 were added in a dilution of 10^7 PFU/ml containing the blocking proteins in the concentrations mentioned above for 12 h at 6°C. Bound virus was detected as in Fig. 5D. For the determination of specific binding, background binding to BSA was subtracted (mean ± standard deviation; $n = 3$). (B) Displacement of LFV bound to α-DG with soluble laminin-1, laminin-2, and fibronectin: Inactivated LFV and LCMV cl-13 (10^7 PFU/ml) were bound to immobilized α-DG. Plates were washed, and the indicated concentrations of ECM proteins were then added for 4 h at room temperature. After three wash steps, bound virus was detected as described in panel A.

the spleen, show limited infection (<10%) of $CD11c^+$ and $DEC205^+$ DC, generate an efficient antiviral T-cell response that clears the infection (46), and are capable of eliciting T- and B-cell responses to other viruses and pathogens. A similar correlation between high α-DG binding affinity, cellular dysfunction, and disease potential was recently discovered in the context of virus-induced inhibition of myelin formation by Schwann cells. LCMV isolates with high α-DG binding affinity efficiently target Schwann cells (infect >98%) and render them incapable of forming myelin sheaths around axons. Low-affinity binders infect Schwann cells to a much lesser degree (<5% of cells) and do not significant impact myelin sheath formation (44).

Immunosuppressive LCMV isolates consistently bind α-DG with affinities in the low-nanomolar range and generally depend on α-DG for infection of cells (31, 46, 49). At the structural level, high-affinity α-DG binding correlated with the presence of an aliphatic amino acid (L or I) in position 260 of GP1 (46). Low-affinity binders generally contain a bulky aromatic amino acid (F) at position 260.

In the present study, we found a high degree of similarity in the receptor binding characteristics between LFV and immunosuppressive isolates of LCMV. Using a combination of virus overlay assay and ELISA-format binding assay, we compared the binding affinities of LFV and the prototypic immunosuppressive LCMV cl-13. Both viruses bound α-DG with affinities in the low-nanomolar range, comparable to the reported binding affinities for α-DG's ECM ligands (56). To study the dependence of LFV infection on α-DG, we generated recombinant VSV containing the GP of LFV in its envelope (VSVΔG*-LFVGP). Our VSV pseudotyped with LFVGP adopted the receptor binding specificity of LFV, as demonstrated by specific blocking of VSVΔG*-LFVGP infection by inactivated LFV. Infection of $DG^{-/-}$ mouse ES cells and their heterozygous $DG^{+/-}$ parental line with VSVΔG*-LFVGP revealed a strong dependence of infection on α-DG. A similar dependence on α-DG for infection has been found for immunosuppressive isolates of LCMV (31, 49) and clade C New World arenaviruses (53).

The similarity in receptor binding between LFV and immunosuppressive LCMV isolates is structurally related, as noted by the conserved binding sites for LFV and LCMV cl-13 on α-DG (30; this study). Binding to both viruses requires structures within parts of the N-terminal globular domain (amino acids 169 to 316) and parts of the central mucin-type domain (amino acids 317 to 408) of α-DG.

At the level of the viral GP, a recent comprehensive comparison of the amino acids in position 260 of GP1 revealed consistently aliphatic residues (L or I) in those arenaviruses that bind α-DG with high affinity (53). The structural conservation and the remarkable similarities in the virus-receptor binding characteristics between LFV and immunosuppressive LCMV isolates indicate a strong evolutionary pressure for high α-DG binding affinity within the Old World arenaviruses.

The ubiquitous expression of α-DG correlates well with the broad tissue tropism of LFV in humans with high viral titers found in spleen, lung, liver, kidney, heart, placenta, and mammary gland (37, 60). Despite the widespread viral replication and development of shock in terminal stages of the disease, histological examination of LF patients shows surprisingly little cellular damage and only a modest or negligible infiltration of inflammatory cells (60). Although hepatic lesions are a consistent pathological change, the degree of hepatic tissue damage is insufficient to cause hepatic failure. Death occurs in the absence of extensive inflammation and tissue destruction, suggesting that the fatal disease is likely caused by virus-induced changes in host cell function, rather than by immune-mediated injury or a direct cytopathic effect of the virus. In the spleen of fatal LFV cases, necrosis occurred predominantly in the marginal zone of the splenic periarteriolar lymphocytic sheath, a finding similar to LCMV cl-13 infection of DCs and the resulting loss of splenic architecture (41, 46, 49). As was shown earlier for LCMV (30, 46, 47, 49), high α-DG binding affinity may also play a crucial role in the ability of LFV to cause immunosuppression. LFV is known to infect DCs in vitro (2, 35), and we postulate that high binding affinity to α-DG may also allow LFV to infect DCs in vivo and alter the antigen presentation function of these cells, resulting in an abortive or inefficient antiviral immune response. The result would thereby favor virus replication and dissemination.

The profound shock associated with fatal LF in humans and primate models without evidence of massive cellular necrosis, vascular thrombosis, or hemorrhage suggests that more subtle changes in vascular function and the blood coagulation system

are likely responsible (37). The observed impairment of vascular function may be due to a direct effect of the virus on the endothelium or due to factors that are released by viral infection of the endothelium or released at a distal site. Based on the pivotal importance of α-DG for normal cell homeostasis and function of different types of vascular endothelial cells (5, 21, 48, 59, 65), the high-affinity interaction of LFV with α-DG may directly contribute to virus-induced alterations underlying the pathogenesis of the vascular leakage and hemorrhagic manifestations of human LF. Experiments are currently under way to test this hypothesis.

Disease outcome in human LF is determined by a close competition between virus spread and the patient's antiviral immune response. Since rapid dissemination of LFV critically depends on its efficient attachment to target cells, which it infects and subsequently replicates in, drugs able to block virus-receptor interaction would give the host's immune system a wider window of opportunity to generate an efficient antiviral immune response. Considering the high binding affinity of LFV to α-DG and its dependence on α-DG for infection, as demonstrated by the present study, α-DG-based recombinant receptor decoys could be used to block virus-host cell attachment. Considering the crucial role of the virus-receptor interaction for initial virus entry, replication, spread, and disease outcome, receptor decoys able to block binding of LFV to target cells, either alone or combined with ribavirin, a drug that inhibits LFV replication (37), might offer the opportunity for better control of LFV than is available at present.

In conclusion, our present study shows that LFV binds α-DG with high affinity and efficiently competes with the interaction of α-DG with its major host-derived ligands, laminins containing laminin α1 and α2 chains. Considering the high expression levels of LFVGP in infected cells and the high viral load associated with late stages of fatal LF, extensive complex formation between α-DG and LFVGP likely occurs. This in turn likely disrupts laminin–α-DG interactions. Perturbation of the laminin–α-DG binding by LFVGP may interfere with α-DG's normal function in cell-matrix adhesion and cellular signaling of crucial cell populations implicated in LF pathogenesis and may therefore contribute to the virus-induced injury observed in fatal LF. The importance of the virus-receptor interaction for virus dissemination and pathogenesis makes it a promising target for the development of novel drugs for treatment of human LFV infection.

ACKNOWLEDGMENTS

This is publication number 16783-NP from the Department of Neuropharmacology, the Scripps Research Institute.

The authors thank Kevin Campbell, Juan-Carlos de la Torre, and Michael J. Buchmeier for reagents and helpful discussions.

This research was supported by Public Health grants AI45927 and AI55540.

REFERENCES

1. **Ahmed, R., A. Salmi, L. D. Butler, J. M. Chiller, and M. B. Oldstone.** 1984. Selection of genetic variants of lymphocytic choriomeningitis virus in spleens of persistently infected mice. Role in suppression of cytotoxic T lymphocyte response and viral persistence. J. Exp. Med. **160:**521–540.
2. **Baize, S., J. Kaplon, C. Faure, D. Pannetier, M. C. Georges-Courbot, and V. Deubel.** 2004. Lassa virus infection of human dendritic cells and macrophages is productive but fails to activate cells. J. Immunol. **172:**2861–2869.
3. **Belkin, A. M., and K. Burridge.** 1995. Association of aciculin with dystrophin and utrophin. J. Biol. Chem. **270:**6328–6337.
4. **Belkin, A. M., and K. Burridge.** 1995. Localization of utrophin and aciculin at sites of cell-matrix and cell-cell adhesion in cultured cells. Exp. Cell Res. **221:**132–140.
5. **Belkin, A. M., and N. R. Smalheiser.** 1996. Localization of cranin (dystroglycan) at sites of cell-matrix and cell-cell contact: recruitment to focal adhesions is dependent upon extracellular ligands. Cell Adhes. Commun. **4:** 281–296.
6. **Borrow, P., and M. B. Oldstone.** 1992. Characterization of lymphocytic choriomeningitis virus-binding protein(s): a candidate cellular receptor for the virus. J. Virol. **66:**7270–7281.
7. **Buchmeier, M. J., M. D. Bowen, and C. J. Peters.** 2001. Arenaviridae: the viruses and their replication, p. 1635–1668. *In* B. N. Fields, D. L. Knipe, and P. M. Howley (ed.), Fields virology. Lippincott-Raven, Philadelphia, Pa.
8. **Cao, W., M. D. Henry, P. Borrow, H. Yamada, J. H. Elder, E. V. Ravkov, S. T. Nichol, R. W. Compans, K. P. Campbell, and M. B. Oldstone.** 1998. Identification of alpha-dystroglycan as a receptor for lymphocytic choriomeningitis virus and Lassa fever virus. Science **282:**2079–2081.
9. **Cavaldesi, M., G. Macchia, S. Barca, P. Defilippi, G. Tarone, and T. C. Petrucci.** 1999. Association of the dystroglycan complex isolated from bovine brain synaptosomes with proteins involved in signal transduction. J. Neurochem. **72:**1648–1655.
10. **Durbeej, M., M. D. Henry, M. Ferletta, K. P. Campbell, and P. Ekblom.** 1998. Distribution of dystroglycan in normal adult mouse tissues. J. Histochem. Cytochem. **46:**449–457.
11. **Dutko, F. J., and M. B. Oldstone.** 1983. Genomic and biological variation among commonly used lymphocytic choriomeningitis virus strains. J. Gen. Virol. **64:**1689–1698.
12. **Ervasti, J. M., and K. P. Campbell.** 1991. Membrane organization of the dystrophin-glycoprotein complex. Cell **66:**1121–1131.
13. **Ervasti, J. M., and K. P. Campbell.** 1993. A role for the dystrophin-glycoprotein complex as a transmembrane linker between laminin and actin. J. Cell Biol. **122:**809–823.
14. **Fisher-Hoch, S. P., O. Tomori, A. Nasidi, G. I. Perez-Oronoz, Y. Fakile, L. Hutwagner, and J. B. McCormick.** 1995. Review of cases of nosocomial Lassa fever in Nigeria: the high price of poor medical practice. Br. Med. J. **311:**857–859.
15. **Freedman, D. O., and J. Woodall.** 1999. Emerging infectious diseases and risk to the traveler. Med. Clin. N. Am. **83:**865–883, v.
16. **Gallaher, W. R., C. DiSimone, and M. J. Buchmeier.** 9 February 2001, posting date. The viral transmembrane superfamily: possible divergence of Arenavirus and Filovirus glycoproteins from a common RNA virus ancestor. BMC Microbiol. **1:**1. [Online.] http://www.biomedcentral.com.
17. **Gee, S. H., F. Montanaro, M. H. Lindenbaum, and S. Carbonetto.** 1994. Dystroglycan-alpha, a dystrophin-associated glycoprotein, is a functional agrin receptor. Cell **77:**675–686.
18. **Henry, M. D., and K. P. Campbell.** 1998. A role for dystroglycan in basement membrane assembly. Cell **95:**859–870.
19. **Henry, M. D., J. S. Satz, C. Brakebusch, M. Costell, E. Gustafsson, R. Fassler, and K. P. Campbell.** 2001. Distinct roles for dystroglycan, beta1 integrin and perlecan in cell surface laminin organization. J. Cell Sci. **114:** 1137–1144.
20. **Holmes, G. P., J. B. McCormick, S. C. Trock, R. A. Chase, S. M. Lewis, C. A. Mason, P. A. Hall, L. S. Brammer, G. I. Perez-Oronoz, M. K. McDonnell et al.** 1990. Lassa fever in the United States. Investigation of a case and new guidelines for management. N. Engl. J. Med. **323:**1120–1123.
21. **Hosokawa, H., H. Ninomiya, Y. Kitamura, K. Fujiwara, and T. Masaki.** 2002. Vascular endothelial cells that express dystroglycan are involved in angiogenesis. J. Cell Sci. **115:**1487–1496.
22. **Ibraghimov-Beskrovnaya, O., J. M. Ervasti, C. J. Leveille, C. A. Slaughter, S. W. Sernett, and K. P. Campbell.** 1992. Primary structure of dystrophin-associated glycoproteins linking dystrophin to the extracellular matrix. Nature **355:**696–702.
23. **Isaacson, M.** 2001. Viral hemorrhagic fever hazards for travelers in Africa. Clin. Infect. Dis. **33:**1707–1712.
24. **James, M., T. M. Nguyen, C. J. Wise, G. E. Jones, and G. E. Morris.** 1996. Utrophin-dystroglycan complex in membranes of adherent cultured cells. Cell Motil. Cytoskelet. **33:**163–174.
25. **James, M., A. Nuttall, J. L. Ilsley, K. Ottersbach, J. M. Tinsley, M. Sudol, and S. J. Winder.** 2000. Adhesion-dependent tyrosine phosphorylation of (beta)-dystroglycan regulates its interaction with utrophin. J. Cell Sci. **113:** 1717–1726.
26. **Johnson, K. M., J. B. McCormick, P. A. Webb, E. S. Smith, L. H. Elliott, and I. J. King.** 1987. Clinical virology of Lassa fever in hospitalized patients. J. Infect. Dis. **155:**456–464.
27. **Kahn, J. S., M. J. Schnell, L. Buonocore, and J. K. Rose.** 1999. Recombinant vesicular stomatitis virus expressing respiratory syncytial virus (RSV) glycoproteins: RSV fusion protein can mediate infection and cell fusion. Virology **254:**81–91.
28. **Kanagawa, M., F. Saito, S. Kunz, T. Yoshida-Moriguchi, R. Barresi, Y. M. Kobayashi, J. Muschler, J. P. Dumanski, D. E. Michele, M. B. Oldstone, and K. P. Campbell.** 2004. Molecular recognition by LARGE is essential for expression of functional dystroglycan. Cell **117:**953–964.

29. **Khurana, T. S., L. M. Kunkel, A. D. Frederickson, S. Carbonetto, and S. C. Watkins.** 1995. Interaction of chromosome-6-encoded dystrophin related protein with the extracellular matrix. J. Cell Sci. **108:**173–185.
30. **Kunz, S., N. Sevilla, D. B. McGavern, K. P. Campbell, and M. B. Oldstone.** 2001. Molecular analysis of the interaction of LCMV with its cellular receptor [alpha]-dystroglycan. J. Cell Biol. **155:**301–310.
31. **Kunz, S., N. Sevilla, J. M. Rojek, and M. B. A. Oldstone.** 2004. Use of alternative receptors different than alpha-dystroglycan by selected isolates of lymphocytic choriomeningitis virus. Virology **325:**432–445.
32. **Lawson, N. D., E. A. Stillman, M. A. Whitt, and J. K. Rose.** 1995. Recombinant vesicular stomatitis viruses from DNA. Proc. Natl. Acad. Sci. USA **92:** 4477–4481.
33. **Lenz, O., J. ter Meulen, H. D. Klenk, N. G. Seidah, and W. Garten.** 2001. The Lassa virus glycoprotein precursor GP-C is proteolytically processed by subtilase SKI-1/S1P. Proc. Natl. Acad. Sci. USA **98:**12701–12705.
34. **Li, S., D. Harrison, S. Carbonetto, R. Fassler, N. Smyth, D. Edgar, and P. D. Yurchenco.** 2002. Matrix assembly, regulation, and survival functions of laminin and its receptors in embryonic stem cell differentiation. J. Cell Biol. **157:**1279–1290.
35. **Mahanty, S., K. Hutchinson, S. Agarwal, M. McRae, P. E. Rollin, and B. Pulendran.** 2003. Cutting edge: impairment of dendritic cells and adaptive immunity by Ebola and Lassa viruses. J. Immunol. **170:**2797–2801.
36. **Matsumura, K., A. Chiba, H. Yamada, H. Fukuta-Ohi, S. Fujita, T. Endo, A. Kobata, L. V. Anderson, I. Kanazawa, K. P. Campbell, and T. Shimizu.** 1997. A role of dystroglycan in schwannoma cell adhesion to laminin. J. Biol. Chem. **272:**13904–13910.
37. **McCormick, J. B., and S. P. Fisher-Hoch.** 2002. Lassa fever. Curr. Top. Microbiol. Immunol. **262:**75–109.
38. **McCormick, J. B., I. J. King, P. A. Webb, K. M. Johnson, R. O′Sullivan, E. S. Smith, S. Trippel, and T. C. Tong.** 1987. A case-control study of the clinical diagnosis and course of Lassa fever. J. Infect. Dis. **155:**445–455.
39. **McCormick, J. B., P. A. Webb, J. W. Krebs, K. M. Johnson, and E. S. Smith.** 1987. A prospective study of the epidemiology and ecology of Lassa fever. J. Infect. Dis. **155:**437–444.
40. **Monath, T. P., V. F. Newhouse, G. E. Kemp, H. W. Setzer, and A. Cacciapuoti.** 1974. Lassa virus isolation from Mastomys natalensis rodents during an epidemic in Sierra Leone. Science **185:**263–265.
41. **Oldstone, M. B.** 2002. Biology and pathogenesis of lymphocytic choriomeningitis virus infection. Curr. Top. Microbiol. Immunol. **263:**83–117.
42. **Parekh, B. S., and M. J. Buchmeier.** 1986. Proteins of lymphocytic choriomeningitis virus: antigenic topography of the viral glycoproteins. Virology **153:**168–178.
43. **Perez, M., M. Watanabe, M. A. Whitt, and J. C. de la Torre.** 2001. N-terminal domain of Borna disease virus G (p56) protein is sufficient for virus receptor recognition and cell entry. J. Virol. **75:**7078–7085.
44. **Rambukkana, A., S. Kunz, J. Min, K. P. Campbell, and M. B. Oldstone.** 2003. Targeting Schwann cells by nonlytic arenaviral infection selectively inhibits myelination. Proc. Natl. Acad. Sci. USA **100:**16071–16076.
45. **Schmitz, H., B. Kohler, T. Laue, C. Drosten, P. J. Veldkamp, S. Gunther, P. Emmerich, H. P. Geisen, K. Fleischer, M. F. Beersma, and A. Hoerauf.** 2002. Monitoring of clinical and laboratory data in two cases of imported Lassa fever. Microbes Infect. **4:**43–50.
46. **Sevilla, N., S. Kunz, A. Holz, H. Lewicki, D. Homann, H. Yamada, K. P. Campbell, J. C. de La Torre, and M. B. Oldstone.** 2000. Immunosuppression and resultant viral persistence by specific viral targeting of dendritic cells. J. Exp. Med. **192:**1249–1260.
47. **Sevilla, N., D. B. McGavern, C. Teng, S. Kunz, and M. B. Oldstone.** 2004. Viral targeting of hematopoietic progenitors and inhibition of DC maturation as a dual strategy for immune subversion. J. Clin. Investig. **113:**737–745.
48. **Shimizu, H., H. Hosokawa, H. Ninomiya, J. H. Miner, and T. Masaki.** 1999. Adhesion of cultured bovine aortic endothelial cells to laminin-1 mediated by dystroglycan. J. Biol. Chem. **274:**11995–12000.
49. **Smelt, S. C., P. Borrow, S. Kunz, W. Cao, A. Tishon, H. Lewicki, K. P. Campbell, and M. B. Oldstone.** 2001. Differences in affinity of binding of lymphocytic choriomeningitis virus strains to the cellular receptor α-dystroglycan correlate with viral tropism and disease kinetics. J. Virol. **75:**448–457.
50. **Sotgia, F., G. Bonuccelli, M. Bedford, A. Brancaccio, U. Mayer, M. T. Wilson, R. Campos-Gonzalez, J. W. Brooks, M. Sudol, and M. P. Lisanti.** 2003. Localization of phospho-beta-dystroglycan (pY892) to an intracellular vesicular compartment in cultured cells and skeletal muscle fibers in vivo. Biochemistry **42:**7110–7123.
51. **Sotgia, F., H. Lee, M. T. Bedford, T. Petrucci, M. Sudol, and M. P. Lisanti.** 2001. Tyrosine phosphorylation of beta-dystroglycan at its WW domain binding motif, PPxY, recruits SH2 domain containing proteins. Biochemistry **40:**14585–14592.
52. **Spence, H. J., A. S. Dhillon, M. James, and S. J. Winder.** 2004. Dystroglycan, a scaffold for the ERK-MAP kinase cascade. EMBO Rep. **5:**484–489.
53. **Spiropoulou, C. F., S. Kunz, P. E. Rollin, K. P. Campbell, and M. B. Oldstone.** 2002. New World arenavirus clade C, but not clade A and B viruses, utilizes α-dystroglycan as its major receptor. J. Virol. **76:**5140–5146.
54. **Sugita, S., F. Saito, J. Tang, J. Satz, K. Campbell, and T. C. Sudhof.** 2001. A stoichiometric complex of neurexins and dystroglycan in brain. J. Cell Biol. **154:**435–445.
55. **Takada, A., C. Robison, H. Goto, A. Sanchez, K. G. Murti, M. A. Whitt, and Y. Kawaoka.** 1997. A system for functional analysis of Ebola virus glycoprotein. Proc. Natl. Acad. Sci. USA **94:**14764–14769.
56. **Talts, J. F., Z. Andac, W. Gohring, A. Brancaccio, and R. Timpl.** 1999. Binding of the G domains of laminin alpha1 and alpha2 chains and perlecan to heparin, sulfatides, alpha-dystroglycan and several extracellular matrix proteins. EMBO J. **18:**863–870.
57. **Tatsuo, H., K. Okuma, K. Tanaka, N. Ono, H. Minagawa, A. Takade, Y. Matsuura, and Y. Yanagi.** 2000. Virus entry is a major determinant of cell tropism of Edmonston and wild-type strains of measles virus as revealed by vesicular stomatitis virus pseudotypes bearing their envelope proteins. J. Virol. **74:**4139–4145.
58. **Teng, M. N., P. Borrow, M. B. A. Oldstone, and J. C. de la Torre.** 1996. A single amino acid change in the glycoprotein of lymphocytic choriomeningitis virus is associated with the ability to cause growth hormone deficiency syndrome. J. Virol. **70:**8438–8443.
59. **Uchino, M., A. Hara, Y. Mizuno, M. Fujiki, T. Nakamura, M. Tokunaga, T. Hirano, T. Yamashita, E. Uyama, Y. Ando, S. Mita, and M. Ando.** 1996. Distribution of dystrophin and dystrophin-associated protein 43DAG (beta-dystroglycan) in the central nervous system of normal controls and patients with Duchenne muscular dystrophy. Intern. Med. **35:**189–194.
60. **Walker, D. H., J. B. McCormick, K. M. Johnson, P. A. Webb, G. Komba-Kono, L. H. Elliott, and J. J. Gardner.** 1982. Pathologic and virologic study of fatal Lassa fever in man. Am. J. Pathol. **107:**349–356.
61. **Weber, E. L., and M. J. Buchmeier.** 1988. Fine mapping of a peptide sequence containing an antigenic site conserved among arenaviruses. Virology **164:**30–38.
62. **Whelan, S. P., L. A. Ball, J. N. Barr, and G. T. Wertz.** 1995. Efficient recovery of infectious vesicular stomatitis virus entirely from cDNA clones. Proc. Natl. Acad. Sci. USA **92:**8388–8392.
63. **Williamson, R. A., M. D. Henry, K. J. Daniels, R. F. Hrstka, J. C. Lee, Y. Sunada, O. Ibraghimov-Beskrovnaya, and K. P. Campbell.** 1997. Dystroglycan is essential for early embryonic development: disruption of Reichert's membrane in Dag1-null mice. Hum. Mol. Genet. **6:**831–841.
64. **Wool-Lewis, R. J., and P. Bates.** 1998. Characterization of Ebola virus entry by using pseudotyped viruses: identification of receptor-deficient cell lines. J. Virol. **72:**3155–3160.
65. **Yamamoto, T., N. Shibata, M. Kanazawa, M. Kobayashi, T. Komori, K. Ikeya, E. Kondo, K. Saito, and M. Osawa.** 1997. Localization of laminin subunits in the central nervous system in Fukuyama congenital muscular dystrophy: an immunohistochemical investigation. Acta Neuropathol. **94:** 173–179.
66. **Yang, B., D. Jung, D. Motto, J. Meyer, G. Koretzky, and K. P. Campbell.** 1995. SH3 domain-mediated interaction of dystroglycan and Grb2. J. Biol. Chem. **270:**11711–11714.